

# Measurement of Vapor–Liquid Equilibria for the Binary Mixture of Propane (R-290) + Isobutane (R-600a)

Jong Sung Lim,<sup>†</sup> Quang Nhu Ho,<sup>‡</sup> Ji-Young Park,<sup>‡</sup> and Byung Gwon Lee<sup>\*‡</sup>

Division of Environmental and Process Technology, Korea Institute of Science and Technology (KIST), P.O. Box 131, Cheongryang, Seoul 130-650, South Korea, and Department of Chemical Engineering, Sogang University, C.P.O. Box 1142, Seoul, South Korea

Isothermal vapor–liquid equilibria data for the binary mixture R-290 + R-600a at four equally spaced temperatures between (273.15 and 303.15) K were measured by using a circulation-type equilibrium apparatus. The experimental data were correlated with the Carnahan–Starling–De Santis equation of state (CSD-EOS) and the Peng–Robinson equation of state (PR-EOS) combined with the Wong–Sandler mixing rule. The data calculated by these equations of state are in good agreement with experimental data. Azeotropic behavior was not found in this mixture.

## Introduction

Chlorofluorocarbons (CFCs) are nontoxic, nonflammable, and nonreactive with other chemical compounds. These preeminent characteristics, along with their good thermodynamic properties, have made them ideal for many applications such as aerosol propellants, electronic cleaning solvents, blowing agents, and special refrigerants for industrial and home refrigeration units. However, they also have a harmful effect on the Earth's protective ozone layer. So they have been regulated internationally by the Montreal Protocol since 1989. Subsequently, it was discovered that CFCs also contributed significantly to the global warming problem. The result was that CFCs have been banned from new applications as of January, 1996. In 2010, the production and use of CFCs will be completely prohibited all over the world.

In consequence, much research has been done to find suitable replacements for CFCs. Initial alternatives included some hydrochlorofluorocarbons (HCFCs), but they will also be phased out around 2030 because their ozone depletion potentials (ODPs) and global warming potentials (GWPs) are relatively high, though they are less than those of CFCs. Hydrofluorocarbons (HFCs)—synthetic refrigerants which have zero ODPs—were proposed as promising replacements for CFCs and HCFCs. Unfortunately, HFCs have significant GWPs (the GWPs of HFCs have been known to be several thousand times higher than that of CO<sub>2</sub>) and have been included in the basket of green house gases to be regulated by the Kyoto Protocol. Furthermore, the manufacture of these HFCs is a high-tech process, and consequently, their cost is high, which would cause a burden for poor countries.

In recent years, the utilization of light hydrocarbons such as propane, *n*-butane, isobutane, propylene, and so forth as effective refrigerants is believed to be an alternative solution because these hydrocarbons are environmentally benign chemicals (zero ODPs and near zero GWPs) and have many outstanding properties. Moreover, they are

common components of natural gas, so they are cheap and plentiful. Their flammability has caused some concerns, but all tests done so far indicated that they are quite safe in small applications such as domestic refrigeration and car air-conditioning, due to the very small amounts involved.<sup>1</sup>

Generally, hydrocarbons can be used as refrigerants in the form of a single component or as a multicomponent mixture. In the case of the second form, vapor–liquid equilibrium data are very important basic information in evaluating the performance of refrigeration cycles and in determining the optimal composition of a mixture. For the mixture of propane (R-290) + isobutane (R-600a), vapor–liquid equilibrium (VLE) data at various temperatures were previously reported by some authors.<sup>2–6</sup> However, some of them were not in detail.

In this work, isothermal VLE data for the binary mixture R-290 + R-600a at four equally spaced temperatures between (273.15 and 303.15) K were measured by using a circulation-type equilibrium apparatus. The experimental data were correlated with the Carnahan–Starling–De Santis equation of state (CSD-EOS) and the Peng–Robinson equation of state (PR-EOS) combined with the Wong–Sandler mixing rule. The interaction parameters and average deviations of pressures and vapor phase compositions obtained from these equations of state are presented. The deviations of other published data from those of the two equations of state above are also reported in this paper.

## Experimental Section

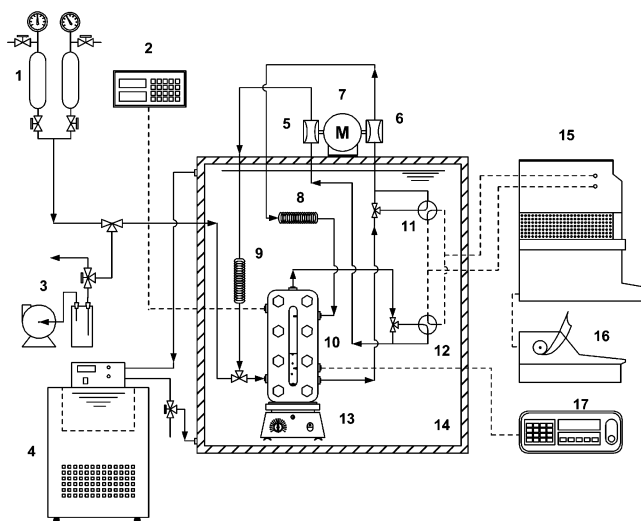
**Chemicals.** High-grade chemicals of propane and isobutane were used for this investigation. Propane of purity higher than 99.5% by mass was supplied by MG Industries, U.S.A. Isobutane supplied by Jeong Il Co., Korea, had a purity higher than 99.8% by mass. The purity of each chemical was validated by using a gas chromatograph.

**Vapor–Liquid Equilibrium Apparatus.** The vapor–liquid equilibrium apparatus used in this work was a circulation-type one in which both liquid and vapor phases were recirculated continuously. The schematic diagram of this apparatus is illustrated in Figure 1. The equilibrium cell (10) was made from type 316 stainless steel with an inner volume of about 85 mL. A pair of Pyrex glass

\* Corresponding author. Telephone: 82-2-958-5857. E-mail address: bglee@kist.re.kr.

<sup>†</sup> Sogang University.

<sup>‡</sup> Korea Institute of Science and Technology (KIST).



- |                              |                                  |
|------------------------------|----------------------------------|
| 1- Sample reservoir          | 2- Pressure indicator            |
| 3- Vacuum pump               | 4- Bath circulator               |
| 5- Vapor circulation pump    | 6- Liquid circulation pump       |
| 7- Electric motor            | 8- Liquid/Liquid heat exchanger  |
| 9- Gas/Liquid heat exchanger | 10- Equilibrium cell             |
| 11- Liquid auto-sampler      | 12- Vapor auto-sampler           |
| 13- Magnetic stirrer         | 14- Bath containing heat carrier |
| 15- Gas chromatograph        | 16- Computing integrator         |
| 17- Temperature indicator    |                                  |

**Figure 1.** Schematic diagram of the vapor–liquid equilibrium apparatus.

windows was installed on two sides of the cell in order to make it possible to observe the inside during operation. Inside the cell, a stirring bar was rotated at variable speeds by an external magnetic stirrer (13), which is used to accelerate the attainment of the equilibrium state and to reduce concentration gradients in both phases.

The temperature of the equilibrium cell in the bath (14) was maintained with a constant temperature heat carrier circulated by using the bath circulator (4) (RCB-20 model manufactured by Jeio Tech, Korea). In the cases when the desired temperature of the cell was higher than 273.15 K, water could be used as heat carrier in this bath. On the contrary, a solution of methanol + water was recommended.

The temperature of the sample in the cell was measured with a platinum resistance sensor connected to a digital temperature indicator (17)—a F250 precision thermometer model manufactured by Automatic Systems Laboratories Ltd., U.K. They were calibrated by an NAMAS accredited calibration laboratory. The total error in the temperature measurements is estimated to be within  $\pm 0.05$  K, including the sensor uncertainty,  $\pm 0.01$  K, the temperature resolution,  $\pm 0.001$  K, and the measurement uncertainty,  $\pm 0.001$  K. The pressure was measured with a pressure transducer, model XPM60, and a digital pressure calibrator indicator (2)—PC106 model manufactured by Beamax, Finland. Pressure calibrations are traceable to national standards (Center for Metrology and Accreditation Certificate Nos. M-95P077 dated 14-11-1995, M-M730 dated 16-11-1995, and M-95P078 dated 16-11-1995),

the calibrator uncertainty was  $\pm 0.0005$  MPa, the sensor uncertainty was  $\pm 0.001$  MPa, and the measurement uncertainty was  $\pm 0.001$  MPa. Thus, the total errors in pressure measurements were estimated to be within  $\pm 0.001$  MPa.

The vapor and liquid phases in the equilibrium cell were continuously recirculated with a dual-head circulation pump, which includes a vapor circulation pump (5) and a liquid circulation pump (6) powered simultaneously by an electric motor (7). This pump was manufactured by the Milton Roy Company, USA. After equilibrium was reached, the vapor and liquid samples were withdrawn from the recycling loop and injected on-line into a Gow-Mac model 550P gas chromatograph (GC) with a vapor autosampler (12) and a liquid one (11). This GC was equipped with a thermal conductivity detector (TCD) and a Porapak Q column from Alltech Company. The signals from the GC were processed and converted to data with a D520B computing integrator (16) supplied by Young In Co., Korea.

**Experimental Procedures.** Experiments to measure VLE data for the binary mixture of R-290 + R-600 at a certain temperature were performed by the following procedure:

The system was first evacuated with a vacuum pump (3) to make sure that all inert gases were removed. An adequate amount of R-600a (less volatile than R-290) contained in the sample reservoir was introduced into the cell, and then the temperature of the entire system was maintained by controlling the temperature of the heat carrier in the bath (14). Note that before the equilibrium state was established, the dual-head pump and stirrer could be turned on just for reducing the time the sample needed to attain that state. After the desired temperature was achieved, the vapor pressure of the R-600a was measured.

Next, a targeted amount of R-290 from the reservoir was supplied into the cell. Both the dual-head pump and stirrer were turned on continuously until the equilibrium state of the mixture in the cell was established. According to our experience, a 1-h period was required to obtain an equilibrium state of the sample in the cell. As soon as the equilibrium state was confirmed, the pressure in the cell was measured and then vapor and liquid samples were withdrawn from the recycling lines by the vapor and liquid autosamplers, respectively. The compositions of the samples were measured by immediately injecting them into the GC, which was connected on-line to the vapor and liquid autosamplers. The GC was calibrated with pure components of known purity and with mixtures of known composition that were prepared gravimetrically. At least three analyses were performed for each phase, and the average value was considered as corresponding to the equilibrium. The composition uncertainty of the composition measurement for both liquid and vapor phases was estimated to be within  $\pm 0.002$  mole fraction.

Finally, the vapor pressure of pure R-290 was measured by the same procedure mentioned above for R-600a.

## Correlation

In this work, the experimental VLE data were correlated with the Carnahan–Starling–De Santis<sup>7</sup> equation of state (CSD-EOS) and the Peng–Robinson equation of state (PR-EOS) combined with the Wong–Sandler mixing rule.

**CSD-EOS.** It was found that the CSD-EOS was able to represent the  $P$ – $V$ – $T$  properties of the halogenated hydrocarbon refrigerants and their mixtures very well. This equation of state is expressed as follows

$$\frac{PV_M}{RT} = \frac{1 + y + y^2 - y^3}{(1 - y)^3} - \frac{a}{RT(V_M + b)} \quad (1)$$

where

$$y = \frac{b}{4V_M} \quad \text{and} \quad V_M \text{ is the molar volume} \quad (2)$$

For a pure component, the temperature dependences of  $a$  and  $b$  are represented by the following forms:

$$a = \alpha_0 \exp(\alpha_1 T + \alpha_2 T^2) \quad (3)$$

$$b = \beta_0 + \beta_1 T + \beta_2 T^2 \quad (4)$$

The CSD-EOS using the approach of Morrison and McLinden<sup>8</sup> was adopted to correlate the VLE data. The coefficients  $\alpha_0$ ,  $\alpha_1$ , and  $\alpha_2$ , in eq 3 and  $\beta_0$ ,  $\beta_1$ , and  $\beta_2$  in eq 4 were cited from REFPROP 5.0.<sup>9</sup>

In the application of the CSD-EOS for a mixture, there exists the effective molecular parameters  $a_m$  and  $b_m$  (the subscript m refers to the mixture) defined by using the following mixing rules:

$$a_m = \sum_{i=1}^n \sum_{j=1}^n x_i x_j a_{ij} \quad (5)$$

$$b_m = \sum_{i=1}^n \sum_{j=1}^n x_i x_j b_{ij} \quad (6)$$

where  $n$  is the number of components in the mixture.

When  $i = j$ , the values of  $a_{ij}$  and  $b_{ij}$  are those of  $a$  and  $b$  for the pure components which are determined by eqs 3 and 4. The values of  $a_{ij}$  and  $b_{ij}$  can be obtained if nearly any experimental property of the mixture is known. For the binary systems, the values of  $a_{12}$  and  $b_{12}$  can be expressed in the following forms:

$$a_{12} = (1 - f_{12})(a_{11}a_{22})^{1/2} \quad (7)$$

$$b_{12} = \frac{1}{8}(b_1^{1/3} + b_2^{1/3})^3 \quad (8)$$

The mixing rule for the  $a$  parameter for the mixture involves the interaction parameter,  $f_{12}$ , which must be determined from experimental data. The approach is to find the value of  $f_{12}$ , which minimizes the sum of square  $\Gamma$  of the relative deviations between measured and calculated quantities,

$$\Gamma(T, x, f_{12}) = \omega_P \left( \frac{P_{\text{exp}} - P_{\text{cal}}}{P_{\text{exp}}} \right)^2 + \omega_L \left( \frac{V_{L, \text{exp}} - V_{L, \text{cal}}}{V_{L, \text{exp}}} \right)^2 + \omega_v \left( \frac{V_{v, \text{exp}} - V_{v, \text{cal}}}{V_{v, \text{exp}}} \right)^2 + \omega_y (y_{\text{exp}} - y_{\text{cal}})^2 \quad (9)$$

Because the vapor composition must be between zero and unity, the last term in eq 9 is expressed as an absolute error. Moreover, experimental data for the vapor and liquid specific volumes indicated in this equation are not available; thus, the corresponding weighting factors in the expression of  $\Gamma$  are set to zero.

$$\Gamma(T, x, f_{12}) = \omega_P \left( \frac{P_{\text{exp}} - P_{\text{cal}}}{P_{\text{exp}}} \right)^2 + \omega_y (y_{\text{exp}} - y_{\text{cal}})^2 \quad (10)$$

**PR-EOS.** The VLE data were corrected with the Peng–Robinson<sup>10</sup> equation of state, which is expressed as follows:

$$P = \frac{RT}{V_M - b} - \frac{a(T)}{V_M(V_M + b) + b(V_M - b)} \quad (11)$$

$$a(T) = \left( 0.457235 \frac{R^2 T_c^2}{P_c} \right) \alpha(T) \quad (12)$$

$$b = 0.077796 \frac{RT_c}{P_c} \quad (13)$$

$$\alpha(T) = [1 + k(1 - \sqrt{TT_c})]^2 \quad (14)$$

$$k = 0.37464 + 1.54226\omega - 0.26992\omega^2 \quad (15)$$

where the parameter  $a$  is a function of temperature,  $b$  is a constant,  $k$  is a constant characteristic of each substance,  $\omega$  is the acentric factor,  $P$  (MPa) is the pressure,  $P_c$  (MPa) is the critical pressure,  $T$  (K) is the absolute temperature,  $T_c$  (K) is the critical temperature,  $T_r$  is the reduced temperature, and  $V_M$  is the molar volume.

The Wong-Sandler<sup>11</sup> mixing rule was used in this work to obtain the equation of state parameters for a mixture from those of the pure components. Wong and Sandler equated the excess Helmholtz free energy at infinite pressure from an equation of state to the excess Helmholtz free energy from any activity coefficient model, in such a way that a mixing rule is obtained which simultaneously satisfies the quadratic composition dependence of the second virial coefficient but also behaves like an activity coefficient model at high density. This mixing rule for a cubic equation of state can be written

$$b_m = \frac{\sum_i \sum_j x_i x_j (b - a/RT)_{ij}}{(1 - A_\infty^E/CRT - \sum_i x_i a_i/RTb_i)} \quad (16)$$

with

$$(b - a/RT)_{ij} = \frac{1}{2}[(b - a/RT)_i + (b - a/RT)_j](1 - k_{ij}) \quad (17)$$

and

$$\frac{a_m}{b_m} = \sum_i x_i \frac{a_i}{b_i} + \frac{A_\infty^E}{C} \quad (18)$$

where  $C$  is a constant equal to  $\ln(\sqrt{2} - 1)/\sqrt{2}$  for the PR-EOS used in this work, and  $k_{ij}$  is the binary interaction parameter. Also,  $A_\infty^E$  is an excess Helmholtz free energy model at infinite pressure which can be equated to a low-pressure excess Gibbs free energy.<sup>12</sup> In this study we use the NRTL model<sup>13</sup> given by

$$\frac{A_\infty^E}{RT} = \sum_i x_i \frac{\sum_j x_j G_{ji} \tau_{ji}}{\sum_r x_r G_{ri}} \quad (19)$$

with

$$G_{ji} = \exp(-\alpha_{ji} \tau_{ji}) \quad \text{and} \quad \tau_{ji} = (g_{ji} - g_{ij})/RT \quad (20)$$

**Table 1. Characteristic Properties of Propane and Isobutane<sup>a</sup>**

characteristic property	propane (R-290)	isobutane (R-600a)
chemical formula	CH <sub>3</sub> CH <sub>2</sub> CH <sub>3</sub>	(CH <sub>3</sub> ) <sub>3</sub> CH
molar mass	44.10	58.12
boiling point, <i>T<sub>b</sub></i> /K	231.06	261.54
critical temperature, <i>T<sub>c</sub></i> /K	369.85	407.85
critical pressure, <i>P<sub>c</sub></i> /MPa	4.248	3.640
critical density, $\rho_c$ /kg·m <sup>-3</sup>	220.5	224.4
acentric factor, $\omega$	0.1524	0.1853

<sup>a</sup> Source: database REFPROP 6.01.<sup>14</sup>

**Table 2. Comparisons of the Vapor Pressures (*P<sub>v</sub>*) of Pure Components between Experimental Data and Data Obtained from the Database REFPROP 6.01<sup>14</sup>**

component	<i>T</i>	<i>P<sub>v,exp</sub></i>	<i>P<sub>v,REF</sub></i>	$\Delta P_v^a$	$\Delta P_v/P_{v,exp}$
	K	MPa	MPa	MPa	%
R-290	273.15	0.4750	0.4743	0.0007	0.147
	283.15	0.6378	0.6364	0.0012	0.188
	293.15	0.8360	0.8362	0.0002	0.024
	303.15	1.0784	1.0790	0.0006	0.056
					avg 0.104
R-600a	273.15	0.1572	0.1564	0.0008	0.509
	283.15	0.2218	0.2201	0.0017	0.766
	293.15	0.3034	0.3018	0.0016	0.527
	303.15	0.4052	0.4043	0.0009	0.222
					avg 0.506

$$^a \Delta P_v = |P_{v,exp} - P_{v,REF}|.$$

where  $G_{ji}$  is the local composition factor for the NRTL model,  $\tau_{ji}$  is the NRTL model binary interaction parameter,  $g_{ji}$  is an interaction energy parameter of the  $i$ - $j$  component,  $\alpha_{ji}$  is a nonrandomness parameter, and  $R$  is the universal gas constant (8.314 J·K<sup>-1</sup>·mol<sup>-1</sup>). The critical properties ( $T_c$ ,  $P_c$ ) and acentric factors ( $\omega$ ) of R-290 and R-600a used to calculate the parameters for the PR-EOS are given in Table 1. We have set the nonrandomness parameter,  $\alpha_{ij}$ , equal to 0.3 for the binary mixture investigated here. The parameters of these equations were obtained by minimizing the following objective function:

$$\text{objective function} = \frac{1}{N} \sum_{i=1}^N \left[ \left( \frac{P_{i,exp} - P_{i,cal}}{P_{i,exp}} \right) \times 100 \right]^2 \quad (21)$$

where  $N$  is the number of experimental points,  $P_{exp}$  is the experimental pressure, and  $P_{cal}$  is the calculated pressure.

## Results and Discussion

Table 1 summarized some characteristic properties of pure R-290 and R-600a from the database REFPROP 6.01,<sup>9</sup> which is considered to be reliable for the pure compounds considered here and consistent with other literature data. The comparison of the saturated vapor pressures ( $P_v$ ) of the pure components between experimental data and calculations obtained from the database REFPROP 6.01 is shown in Table 2, which shows that the absolute deviations of vapor pressure for both R-290 and R-600a were within  $\pm 0.002$  MPa and the average relative deviations ( $\Delta P_v/P_v$ ) from the REFPROP database were 0.10% for R-290 and 0.51% for R-600a.

The experimental VLE data for the binary mixture R-290 + R-600a, including the mole fractions of R-290 in the liquid and vapor phases and the pressures in equilibrium at 273.15, 283.15, 293.15, and 303.15 K, are listed in Table 3. The VLE data calculated by the CSD-EOS and PR-EOS and their deviations in pressure ( $\Delta P/P_{exp}$ ) and deviations

**Table 3. Experimental Vapor–Liquid Equilibrium Data at Various Temperatures for the Mixture of R-290 (1) + R-600a (2)**

<i>T</i> /K	<i>x</i> <sub>1,exp</sub>	<i>y</i> <sub>1,exp</sub>	<i>P</i> <sub>exp</sub> /MPa	<i>T</i> /K	<i>x</i> <sub>1,exp</sub>	<i>y</i> <sub>1,exp</sub>	<i>P</i> <sub>exp</sub> /MPa
273.15	0.000	0.000	0.1572	293.15	0.000	0.000	0.3034
	0.092	0.205	0.1849		0.115	0.233	0.3610
	0.198	0.390	0.2156		0.286	0.469	0.4405
	0.284	0.506	0.2416		0.390	0.586	0.4950
	0.385	0.617	0.2720		0.514	0.706	0.5627
	0.488	0.708	0.3046		0.596	0.768	0.6085
	0.586	0.781	0.3386		0.701	0.845	0.6660
	0.697	0.850	0.3729		0.780	0.886	0.7109
	0.799	0.906	0.4070		0.859	0.929	0.7548
	0.898	0.955	0.4403		0.935	0.970	0.8009
283.15	1.000	1.000	0.4750	303.15	1.000	1.000	0.8360
	0.000	0.000	0.2218		0.000	0.000	0.4052
	0.085	0.182	0.2547		0.119	0.226	0.4770
	0.239	0.429	0.3110		0.220	0.385	0.5407
	0.321	0.531	0.3465		0.332	0.517	0.6086
	0.405	0.617	0.3811		0.441	0.625	0.6802
	0.517	0.708	0.4234		0.535	0.716	0.7449
	0.606	0.782	0.4624		0.621	0.780	0.8098
	0.697	0.843	0.5058		0.706	0.840	0.8682
	0.792	0.894	0.5468		0.802	0.895	0.9372
0.908	0.955	0.5964	0.900	0.949	1.0063		
1.000	1.000	0.6378	1.000	1.000	1.0784		

in vapor phase compositions ( $\delta y_1$ ) compared with experimental data at various temperatures are given in Tables 4 and 5. The interaction parameters and the average deviations in pressure (AD- $P$ ) and average deviations in vapor phase compositions (AD- $y_1$ ) between measured and calculated values for the mixture of R-290 + R-600a are reported in Table 6. The values of  $f_{12}$  determined at (273.15, 283.15, 293.15, and 303.15) K were  $-0.0044$ ,  $-0.0039$ ,  $-0.0049$ , and  $-0.0015$ , respectively, for the CSD-EOS and 0.0342, 0.0317, 0.13575, and 0.0530, respectively, for the PR-EOS.

The  $P$ - $x$ - $y$  diagrams for the mixture R-290 + R-600a at various temperatures are shown in Figure 2, where the experimental VLE data at (273.15, 283.15, 293.15, and 303.15) K are shown as closed circles, triangles, squares, and diamonds, respectively. The black dashed lines represent the calculated data by the CSD-EOS (Figure 2a) or by the PR-EOS (Figure 2b). Both experimental and calculated  $P$ - $x$ - $y$  diagrams indicate that azeotropic behavior was not found in this mixture in the range of temperatures between (273.15 and 303.15) K, and the calculated diagrams did not coincide accurately with the corresponding experimental values. This difference can be demonstrated clearly by the deviations of vapor phase compositions and pressures of calculated data compared with experimental values at each point, which are shown in Figures 3 and 4. However, the results of the comparison showed that the values of AD- $P$  calculated by the CSD-EOS and by the PR-EOS varied within 0.26–0.47% and 0.29–0.53%, respectively. Also, the AD- $y$  varied within 0.005 to 0.011 for the CSD-EOS and 0.007 to 0.013 for the PR-EOS. All values are relatively low and acceptable. In other ways, the data calculated by using the CSD-EOS or the PR-EOS give good agreement with the experimental data in this range of temperature between (273.15 and 303.15) K.

For the mixture of R-290 + R-600a, VLE data at various temperatures were previously reported by some authors. Their average deviations from the CSD-EOS and the PR-EOS are summarized in Table 7. In the same range of temperatures we investigated, particularly at (283.15, 293.15, and 303.15) K, some data were also presented by Higashi et al.<sup>2</sup> However, the deviations of these data were somewhat higher than those of our experimental data: the values of AD- $P$  and AD- $y$  were within 1.38–2.62% and

**Table 4. Deviations of Pressures and Vapor Phase Compositions Calculated from the CSD-EOS for the Mixture of R-290 (1) + R-600a (2) at Various Temperatures**

<i>T</i> /K	$x_{1,\text{exp}}$	$P_{\text{CSD}}/\text{MPa}$	$(\Delta P_{\text{CSD}}/P_{\text{exp}})/\%^a$	$y_{1,\text{CSD}}$	$\delta y_{1,\text{CSD}}^b$
273.15	0.000	0.1567	0.301	0.000	0.000
	0.092	0.1836	0.694	0.217	0.012
	0.198	0.2151	0.241	0.402	0.012
	0.284	0.2411	0.200	0.519	0.013
	0.385	0.2720	0.003	0.629	0.013
	0.488	0.3043	0.095	0.721	0.013
	0.586	0.3359	0.784	0.794	0.012
	0.697	0.3720	0.229	0.862	0.012
	0.799	0.4063	0.182	0.916	0.010
	0.898	0.4398	0.111	0.960	0.005
1.000	0.4749	0.015	1.000	0.000	
283.15	0.000	0.2201	0.781	0.000	0.000
	0.085	0.2523	0.953	0.192	0.010
	0.239	0.3124	0.461	0.446	0.016
	0.321	0.3450	0.423	0.547	0.016
	0.405	0.3792	0.488	0.634	0.017
	0.517	0.4254	0.479	0.731	0.023
	0.606	0.4630	0.130	0.796	0.014
	0.697	0.5019	0.767	0.853	0.010
	0.792	0.5438	0.544	0.906	0.012
	0.908	0.5958	0.108	0.962	0.007
1.000	0.6377	0.010	1.000	0.000	
293.15	0.000	0.3014	0.672	0.000	0.000
	0.115	0.3563	1.293	0.237	0.004
	0.286	0.4414	0.195	0.489	0.020
	0.390	0.4947	0.069	0.604	0.017
	0.514	0.5608	0.346	0.716	0.010
	0.596	0.6049	0.596	0.778	0.009
	0.701	0.6637	0.339	0.848	0.003
	0.780	0.7084	0.352	0.894	0.007
	0.859	0.7542	0.077	0.935	0.006
	0.935	0.7992	0.206	0.971	0.002
1.000	0.8385	0.297	1.000	0.000	
303.15	0.000	0.4036	0.389	0.000	0.000
	0.119	0.4776	0.119	0.237	0.011
	0.220	0.5419	0.214	0.393	0.007
	0.332	0.6138	0.851	0.530	0.013
	0.441	0.6860	0.850	0.640	0.015
	0.535	0.7489	0.542	0.720	0.004
	0.621	0.8081	0.212	0.784	0.004
	0.706	0.8670	0.143	0.841	0.001
	0.802	0.9354	0.192	0.898	0.003
	0.900	1.0069	0.059	0.951	0.002
1.000	1.0820	0.335	1.000	0.000	

$$^a \Delta P_{\text{CSD}} = |P_{\text{exp}} - P_{\text{CSD}}|, \quad ^b \delta y_{1,\text{CSD}} = |y_{1,\text{exp}} - y_{1,\text{CSD}}|.$$

0.013–0.025 of those from the CSD-EOS, and they were within 0.73–1.80% and 0.008–0.039 of those from the PR-EOS, respectively. It was also found that the previous data at other temperatures showed relatively different deviations (especially deviations in pressure) from the CSD-EOS and the PR-EOS. In the case of the VLE data between (237.18 and 339.73) K reported by Hipkin et al.<sup>3</sup> or Hirata et al.,<sup>4,5</sup> the values of AD- $y$  were rather small, within 0.004 to 0.020 to both two equations of state; meanwhile, the values of AD- $P$  were still high (1.04 to 3.8)%—compared to those of the CSD-EOS and acceptable (0.29 to 1.01%)—compared to those of the PR-EOS. However, the VLE data recently presented by Holcomb et al.<sup>6</sup> showed that the values calculated by using either the CSD-EOS or the PR-EOS give good agreement with the experimental data in the range of temperatures between (250.0 and 385.0) K; for example, most of the values of AD- $P$  and AD- $y$  varied within (0.26 to 0.60)% and 0.001 to 0.02, respectively.

## Conclusions

Measurements of the vapor–liquid equilibria for the mixture of R-290 + R-600a at four equally spaced temper-

**Table 5. Deviations of Pressures and Vapor Phase Compositions Calculated from the PR-EOS for the Mixture of R-290 (1) + R-600a (2) at Various Temperatures**

<i>T</i> /K	$x_{1,\text{exp}}$	$P_{\text{PR}}/\text{MPa}$	$(\Delta P_{\text{PR}}/P_{\text{exp}})/\%^a$	$y_{1,\text{PR}}$	$\delta y_{1,\text{PR}}^b$
273.15	0.000	0.1565	0.426	0.000	0.000
	0.092	0.1838	0.600	0.219	0.015
	0.198	0.2157	0.033	0.406	0.016
	0.284	0.2420	0.157	0.523	0.017
	0.385	0.2731	0.401	0.633	0.016
	0.488	0.3055	0.279	0.724	0.016
	0.586	0.3369	0.490	0.796	0.014
	0.697	0.3727	0.064	0.863	0.013
	0.799	0.4063	0.172	0.916	0.010
	0.898	0.4392	0.259	0.960	0.005
1.000	0.4735	0.312	1.000	0.000	
283.15	0.000	0.2218	0.929	0.000	0.000
	0.085	0.2547	0.931	0.194	0.012
	0.239	0.3110	0.682	0.449	0.020
	0.321	0.3465	0.159	0.550	0.019
	0.405	0.3811	0.213	0.638	0.021
	0.517	0.4234	0.718	0.734	0.026
	0.606	0.4624	0.301	0.798	0.016
	0.697	0.5058	0.692	0.854	0.011
	0.792	0.5468	0.593	0.906	0.013
	0.908	0.5964	0.315	0.961	0.006
1.000	0.6378	0.336	1.000	0.000	
293.15	0.000	0.3034	0.831	0.000	0.000
	0.115	0.3610	0.047	0.242	0.009
	0.286	0.4405	0.175	0.487	0.018
	0.390	0.4950	0.139	0.606	0.019
	0.514	0.5627	0.064	0.723	0.017
	0.596	0.6085	0.107	0.786	0.017
	0.701	0.6660	0.210	0.854	0.009
	0.780	0.7109	0.066	0.897	0.011
	0.859	0.7548	0.099	0.936	0.008
	0.935	0.8009	0.300	0.971	0.002
1.000	0.8360	0.001	1.000	0.000	
303.15	0.000	0.4052	0.538	0.000	0.000
	0.119	0.4770	0.361	0.237	0.010
	0.220	0.5407	0.309	0.394	0.009
	0.332	0.6086	0.398	0.533	0.016
	0.441	0.6802	0.507	0.644	0.019
	0.535	0.7449	0.286	0.724	0.008
	0.621	0.8098	0.410	0.788	0.008
	0.706	0.8682	0.313	0.844	0.004
	0.802	0.9372	0.360	0.900	0.005
	0.900	1.0063	0.127	0.952	0.002
1.000	1.0784	0.130	1.000	0.000	

$$^a \Delta P_{\text{PR}} = |P_{\text{exp}} - P_{\text{PR}}|, \quad ^b \delta y_{1,\text{PR}} = |y_{1,\text{exp}} - y_{1,\text{PR}}|.$$

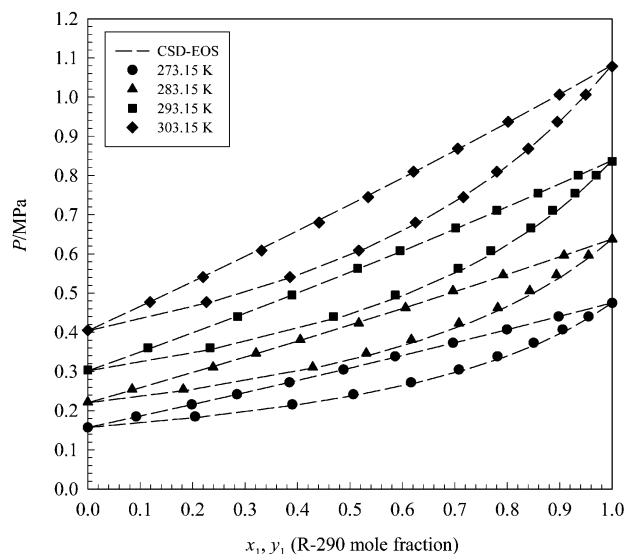
**Table 6. Interaction Parameters ( $f_{12}$ ,  $k_{12}$ ), Average Deviations of Pressures (AD- $P$ ), and Average Deviations of Vapor Phase Compositions (AD- $y$ ) for the Mixture of R-290 (1) + R-600a (2) at Various Temperatures**

<i>T</i> /K	CSD-EOS			PR-EOS		
	$f_{12}$	AD- $P^a/\%$	AD- $y^b$	$k_{12}$	AD- $P^a/\%$	AD- $y^b$
273.15	−0.0044	0.260	0.009	0.034 24	0.290	0.010
283.15	−0.0039	0.468	0.011	0.031 67	0.533	0.013
293.15	−0.0049	0.404	0.007	0.135 75	0.185	0.010
303.15	−0.0015	0.355	0.005	0.053 03	0.340	0.007

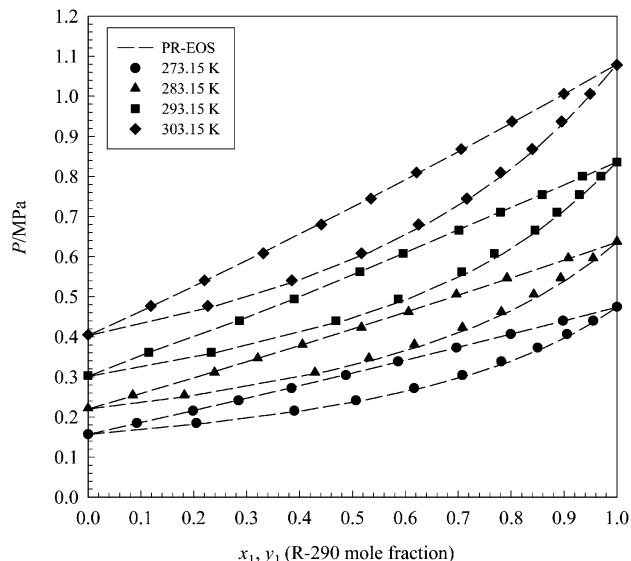
$$^a \text{AD-}P = 1/N \sum_{i=1}^N (\Delta P_i / P_{\text{exp},i} \times 100), \quad ^b \text{AD-}y = 1/N \sum_{i=1}^N (\delta y_{1,i}).$$

atures between (273.15 and 303.15) K were carried out by using a circulation-type equilibrium apparatus. It was found that this mixture did not show azeotropic behavior over this range of temperature.

The experimental VLE data were correlated with the CSD-EOS and the PR-EOS combined with the Wong–Sandler mixing rule. The calculated data obtained from these equations of state show good agreement with the experimental values. This result indicates that both the CSD-EOS and the PR-EOS can be used to estimate the

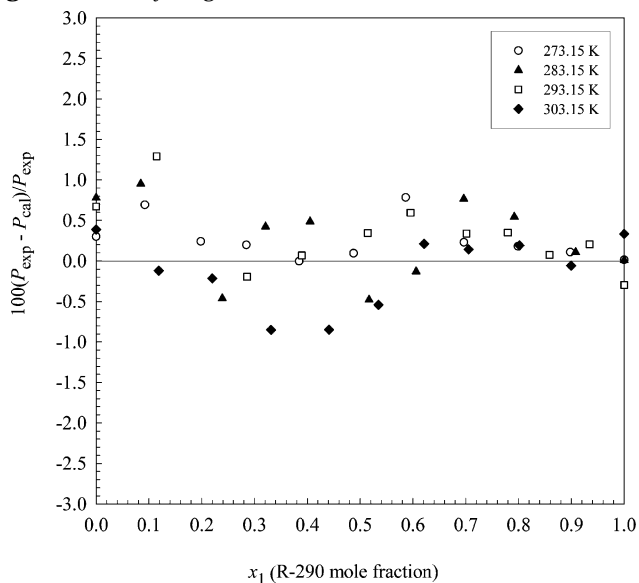


(a) Experimental data and data calculated from CSD-EOS

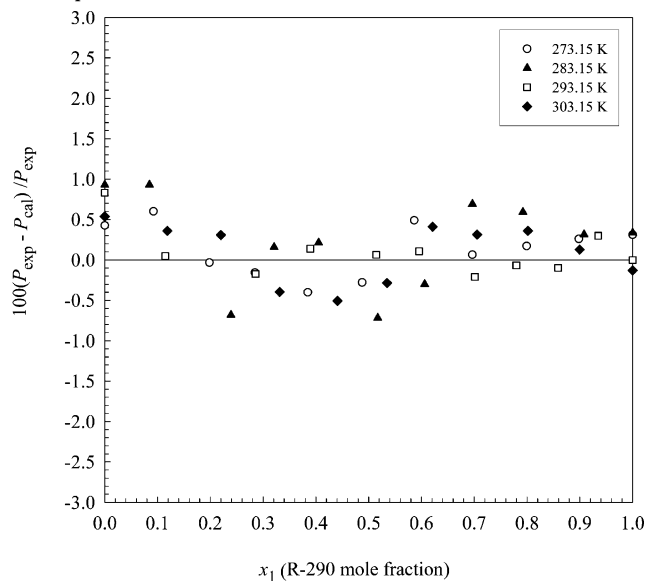


(b) Experimental data and data calculated from PR-EOS

**Figure 2.**  $P$ - $x$ - $y$  diagram for the mixture R-290 + R-600a at various temperatures.

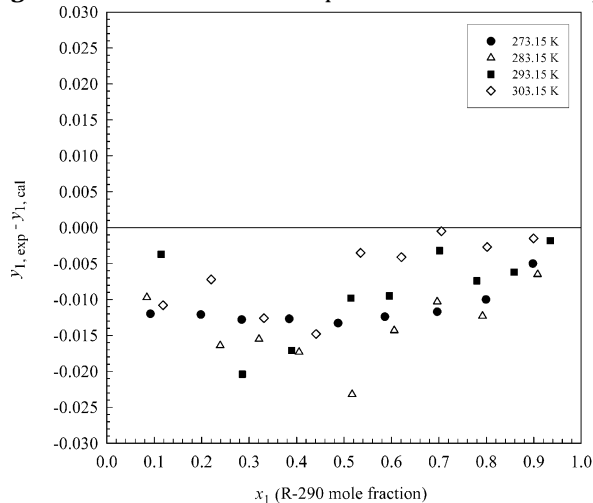


(a) Deviations of calculated pressures obtained from the CSD-EOS

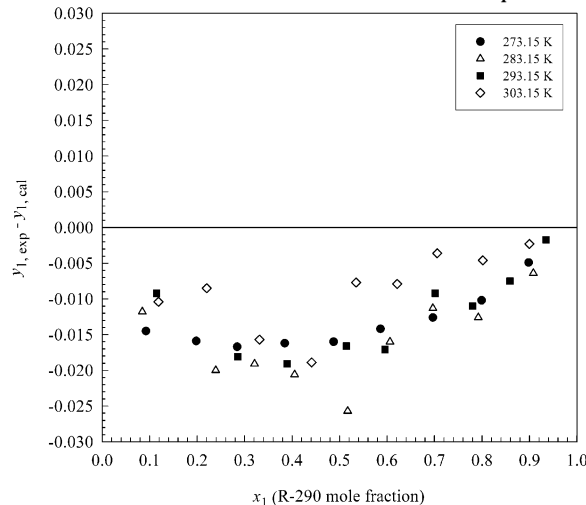


(b) Deviations of calculated pressures obtained from the PR-EOS

**Figure 3.** Deviations between experimental and calculated pressures for the mixture R-290 + R-600a at various temperatures.



(a) Deviations of calculated vapor phase compositions obtained from the CSD-EOS



(b) Deviations of calculated vapor phase compositions obtained from the PR-EOS

**Figure 4.** Deviations between experimental and calculated vapor phase compositions for the mixture R-290 + R-600a at various temperatures.

**Table 7. Deviations of Published Data<sup>2-6</sup> from those of the CSD-EOS and the PR-EOS for the Mixture of R-290 + R-600a at Various Temperatures**

<i>T</i> /K	CSD-EOS		PR-EOS	
	AD- <i>P</i> %	AD- <i>y</i>	AD- <i>P</i> %	AD- <i>y</i>
283.15 <sup>a</sup>	2.612	0.025	1.796	0.039
293.15 <sup>a</sup>	1.579	0.022	0.731	0.026
303.15 <sup>a</sup>	1.379	0.015	0.808	0.008
313.15 <sup>a</sup>	1.768	0.013	1.441	0.020
266.54 <sup>b</sup>	3.827	0.009	0.292	0.006
299.80 <sup>b</sup>	1.550	0.006	1.086	0.007
338.679 <sup>b</sup>	1.381	0.010	0.563	0.011
366.457 <sup>b</sup>	1.038	0.004	0.545	0.016
237.18 <sup>c</sup>	4.818	0.007	1.073	0.020
249.17 <sup>c</sup>	2.700	0.016	0.865	0.016
339.73 <sup>d</sup>	3.148	0.013	0.585	0.004
250.0 <sup>e</sup>	0.568	0.001	0.350	0.005
270.0 <sup>e</sup>	0.442	0.006	0.289	0.018
290.0 <sup>e</sup>	0.378	0.007	0.259	0.003
310.0 <sup>e</sup>	0.737	0.007	0.467	0.019
330.0 <sup>e</sup>	0.380	0.015	0.405	0.045
350.0 <sup>e</sup>	0.450	0.009	0.466	0.016
375.0 <sup>e</sup>	0.370	0.005	0.451	0.003
385.0 <sup>e</sup>	0.579	0.007	0.702	0.008

<sup>a</sup> Reference 2. <sup>b</sup> Reference 3. <sup>c</sup> Reference 4. <sup>d</sup> Reference 5. <sup>e</sup> Reference 6.

thermodynamic properties for the binary mixture R-290 + R-600a in the range of temperatures between (273.15 and 303.15) K and can be applied to other ranges, but additional experiments are needed to confirm this.

### List of Symbols

$A_{\infty}^E$  = excess Helmholtz free energy  
 $a(a_{ij})$  = equation of state attraction parameter (between species  $i$  and  $j$ )  
 $b(b_{ij})$  = equation of state volume parameter (between species  $i$  and  $j$ )  
 $b$  = a constant  
 $C$  = numerical constant equal to  $\ln(\sqrt{2} - 1)/\sqrt{2}$  for the PR-EOS  
 $f_{12}, k_{12}$  = interaction parameter between species 1 and 2  
 $g_{ij}$  = interaction energy parameter of the  $i$ - $j$  component  
 $G_{ij}$  = local composition factor for the NRTL model  
 $k$  = constant characteristic of each substance  
 $n$  = number of components in a mixture  
 $N$  = number of experiments  
 $P, P_c, P_v$  = pressure, critical pressure, vapor pressure (MPa)  
 $R$  = gas constant,  $R = 8.3144$  (J·mol<sup>-1</sup>·K<sup>-1</sup>)  
 $T, T_c$  = absolute temperature, critical temperature (K)  
 $T_r$  = reduced temperature  
 $T_s$  = boiling point at 1 atm (K)  
 $V, V_M$  = total volume, molar volume  
 $x$  = mole fraction in liquid phase  
 $y$  = mole fraction in vapor phase  
 $y = b/4V_M$

### Greek Letters

$\alpha(T)$  = temperature dependent  
 $\alpha_0, \alpha_1, \alpha_2$  = coefficients for the temperature independence of  $a$

$\beta_0, \beta_1, \beta_2$  = coefficients for the temperature independence of  $b$

$\Delta, \delta$  = change in a quantity

$\omega$  = acentric factor

$\omega_L$  = weighting factor for liquid volume

$\omega_P$  = weighting factor for saturation pressure

$\omega_v$  = weighting factor for vapor volume

$\omega_y$  = weighting factor for vapor phase composition

### Subscripts

avg = average

c = critical property

cal = calculated

exp = experimental

$i, j$  =  $i$ th,  $j$ th component of the mixture

l = liquid phase

m = mixture

v = vapor phase

REF = REFPROP

### Literature Cited

- (1) Aisbeet, E.; Pham, T. Natural Replacements for Ozone-Depleting Refrigerants in Eastern and Southern Asia, Seminar on Environment and Development in Vietnam, National Center for Development Studies, Australian National University, Dec 6-7, 1996.
- (2) Higashi, Y.; Funakura, M.; Yoshida, Y. Vapor-Liquid Equilibrium for Propane/Isobutane Mixture, Proc. International Conference: "CFC, The Day After", Padova, Italy, 1994; pp 493-500.
- (3) Hipkin, H. Experimental Vapor-Liquid Equilibrium Data for Propane-Isobutane. *AIChE J.* **1996**, *12*, 484-487.
- (4) Hirata, M.; Suda, S.; Hakuta, T.; Nagahama, K. Light Hydrocarbon Vapor-Liquid Equilibria. *Mem. Fac. Technol., Tokyo Metropol. Univ.* **1969**, *19*, 103-122.
- (5) Hirata, M.; Suda, S.; Miyashita, R.; Hoshino, T. High-Pressure Vapor-Liquid Equilibria. Experimental Data on the System Propane-Isobutane at 66.60 °C. *Mem. Fac. Technol., Tokyo Metropol. Univ.* **1970**, *20*, 1811-1817.
- (6) Holcomb, C. D.; Outcalt, S. L. Design of a Vapor-Liquid Equilibrium, Surface Tension, and Density Apparatus, Proceedings of the 15<sup>th</sup> Symposium on Energy and Engineering Sciences, Argonne, IL, 1997, pp 23-30.
- (7) De Santis, R.; Gironi, F.; Marrelli, L. Vapor-Liquid Equilibrium from Hard-Sphere Equation of State. *Ind. Eng. Chem. Fundam.* **1976**, *15*, 183-189.
- (8) Morrison, G.; McLinden, M. O. *Application of a Hard Sphere Equation of State to Refrigerants and Refrigerant Mixtures*, National Bureau of Standards and Technology Note 1226; U.S.A., 1986.
- (9) Huber, M.; Gallagher, J.; McLinden, M.; Morrison, G. *NIST Thermodynamic and Transport Properties of Refrigerants and Refrigerant Mixtures Database (REFPROP)*, Ver. 5.0; National Bureau of Standards and Technology: Boulder, CO, 1998.
- (10) Peng, D. Y.; Robinson, D. B. A New Two-Constant Equation of State. *Ind. Eng. Chem. Fundam.* **1976**, *15*, 59-64.
- (11) Wong, D. S. H.; Sandler, S. I. A Theoretically Correct Mixing Rule for Cubic Equations of State. *AIChE J.* **1992**, *38*, 671-680.
- (12) Wong, D. S. H.; Orbey, H.; Sandler, S. I. Equation of State Mixing Rule for Nonideal Mixtures Using Available Activity Coefficient Model Parameter and That allows Extrapolation over Large Ranges of Temperature and Pressure. *Ind. Eng. Chem. Res.* **1992**, *31*, 2033-2039.
- (13) Renon, H.; Prausnitz, J. M. Local Compositions in Thermodynamic Excess Functions for Liquid Mixtures. *AIChE J.* **1968**, *14*, 135-144.
- (14) McLinden, M. O.; Klein, S. A.; Lemmon, E. W.; Peskin, A. P. *Thermodynamic Properties of Refrigerants and Refrigerant Mixtures Database (REFPROP)*, Ver. 6.01; NIST: Boulder, CO, 1998.

Received for review January 1, 2003. Accepted November 1, 2003.

JE030106K